Biochemical and Biophysical Research Communications 434 (2013) 746–752

Contents lists available at SciVerse ScienceDirect

Biochemical and Biophysical Research Communications

journal homepage: www.elsevier.com/locate/ybbrc

Overexpression of miR-21 in patients with ulcerative colitis impairs intestinal epithelial barrier function through targeting the Rho GTPase RhoB

Yongzhi Yang [a], Yanlei Ma [b], Chenzhang Shi [a], Hongqi Chen [a], Huizhen Zhang [c], Niwei Chen [d], Peng Zhang [b], Feng Wang [b], Jun Yang [a], Jianjun Yang [a], Qingchao Zhu [a], Yong Liang [a], Wen Wu [a], Renyuan Gao [a], Zhe Yang [a], Yang Zou [a,*], Huanlong Qin [b,*]

[a] Department of Surgery, The Sixth People's Hospital Affiliated to Shanghai Jiao Tong University, 600 Yishan Road, Shanghai 200233, PR China
[b] Department of General Surgery, Shanghai Tenth People's Hospital Affiliated to Tongji University, 301 Yanchang Road, Shanghai 200072, PR China
[c] Department of Pathology, The Sixth People's Hospital Affiliated to Shanghai Jiao Tong University, Shanghai 200233, PR China
[d] Department of Gastroenterology, The Sixth People's Hospital Affiliated to Shanghai Jiao Tong University, Shanghai 200233, PR China

ARTICLE INFO

Article history:
Received 18 March 2013
Available online 10 April 2013

Keywords:
Ulcerative colitis
miR-21
Intestinal epithelial barrier
RhoB

ABSTRACT

Although epithelial barrier dysfunction in the gut has been extensively reported in ulcerative colitis (UC), the pathogenesis of this disease is not completely understood. In the present study, we investigated the role of miR-21 in regulating intestinal epithelial barrier function in UC. Colonic biopsies were obtained from 30 chronic UC patients and 30 healthy controls. Using real-time quantitative polymerase chain reaction (qRT-PCR), we found that both the mucosal and serum levels of miR-21 were upregulated in UC. *In situ* hybridization (ISH) analysis confirmed the accumulation of miR-21 in UC epithelia cells *in vivo*. Immunohistochemistry, Western Blot, qRT-PCR, and ultrastructural analyses further demonstrated that the overexpression of miR-21 in UC mucosa and Caco-2 cells impaired the integrity of the tight junctions, resulted in a decrease of the transepithelial electrical resistance (TER) and an increase of the inulin permeability. Furthermore, miR-21 induced the degradation of RhoB mRNA, which led to the depletion of RhoB and the impairment of tight junctions in intestinal epithelial cells.

1. Introduction

Inflammatory bowel disease (IBD) is a group of chronic, idiopathic, relapsing, and remitting immune dysregulation disorders of the gastrointestinal tract in genetically susceptible individuals who are exposed to environmental risk factors [1,2]. IBD is typically classified as ulcerative colitis (UC) or Crohn's disease (CD). A steady increase in the incidence and prevalence of UC has occurred over the past two decades [3]. Although epithelial barrier dysfunction in the gut has been extensively reported in UC, the pathogenesis of this disease is not completely understood [4,5].

MicroRNAs (miRNAs) are short non-coding RNAs that have emerged as key modulators of various cellular processes at the post-transcriptional level [6]. miR-21 is highly expressed in almost all types of cancer and has been reported to be involved in inflammation [7,8]. Sheedy et al. [7] reported that miR-21 acts as a negative regulator of Toll-like receptor 4 (TLR4) signaling by targeting the proinflammatory protein PDCD4. Wu et al. [9] identified miR-21 as one of the most highly expressed miRNAs associated with active UC. Takagi et al. [10] confirmed that miR-21 levels were elevated in inflamed tissues. Despite several studies investigating the role of miR-21 in IBD, the functions of miR-21 in the intestinal epithelial barrier, which plays a pivotal role in the etiology and pathogenesis of IBD, remain to be defined. The purpose of this study was to investigate the role of miR-21 in regulating the function of the intestinal epithelial barrier in UC.

2. Materials and methods

2.1. Clinical samples

Between 2010 and 2011, colonic biopsies were obtained from 30 chronic UC patients (cohort 1, 7 male and 8 female patients, mean age of 39.4 years, range of 20–65 years; cohort 2, 9 male and 6 female patients, mean age of 48.5 years, range of 22–67 years) from the Department of Gastrointestinal Endoscopy, the Sixth People's Hospital Affiliated to Shanghai Jiao Tong University. Biopsy specimens were collected from 30 healthy control patients (cohort 1, 8 male and 7 female patients, median age of 44.5 years, range of 23–67 years; cohort 2, 9 male and 6 female patients, median age of 50.7 years, range of 26–70 years) undergoing

* Corresponding authors. Fax: +86 21 66300588 (H. Qin), fax: +86 21 64368920 (Y. Zou).
E-mail addresses: yangzoush@hotmail.com (Y. Zou), hl-qin@hotmail.com (H. Qin).

0006-291X/$ - see front matter © 2013 Elsevier Inc. All rights reserved.
http://dx.doi.org/10.1016/j.bbrc.2013.03.122

Table 1
Clinical characteristics of patients.

	Cohort 1		Cohort 2	
	Control	UC	Control	UC
Total (n)	15	15	15	15
Male/Female (n)	8/7	7/8	9/6	9/6
Age (y)				
Mean	44.5	39.4	50.7	48.5
Range	23–67	20–65	26–70	22–67
Extent of colitis (n)				
Left-sided	NA	6	NA	6
Pancolitis		9		9
Disease duration (y)				
Mean	NA	12.6	NA	14.6
Range		6–25		5–24
Medications (n)				
5-ASA	0	14	0	13
Steroid treatment	0	5	0	6
Immunomodulator	0	7	0	8
Antibiotics	0	4	0	2
Probiotics	0	8	0	8

UC, ulcerative colitis; n, number; y, year; NA, not applicable.

a colonoscopy for UC exclusion; these patients did not show inflammation either macroscopically or microscopically. Written consent was obtained from all subjects prior to the procedures. The clinicopathological data included age, gender, extent of colitis, disease duration, and medications. To maximize RNA and protein extraction, we adopted the strategy of using two cohorts that both included 15 healthy controls and 15 UC individuals. We performed qRT-PCR and immunohistochemistry on the samples from cohort 1, whereas Western Blot analysis and *in situ* hybridization were performed on the samples from cohort 2. The clinical characteristics of each group are listed in Table 1. The Ethics Committee of the Sixth People's Hospital Affiliated to Shanghai Jiao Tong University approved this project.

2.2. Immunohistochemistry

Formalin-fixed paraffin-embedded (FFPE) colonic biopsy sections were dewaxed in xylene and rehydrated. To block endogenous peroxidase activity, the slides were treated with methanol containing 0.3% hydrogen peroxide for 10 min. After washing in Tris buffer, the slides were incubated for 30 min at 37 °C with primary antibodies against the following proteins: RhoB (rabbit polyclonal, diluted 1:150; Abcam, Cambridge, UK), occludin (rabbit monoclonal, diluted 1:150; Cell Signaling Technology, MA, USA), and zonula occludens-1 (ZO-1, goat polyclonal, diluted 1:150; Santa Cruz Biotechnology, CA, USA). Peroxidase-conjugated secondary antibodies were used for immunostaining. The peroxidase activity was visualized using the 3, 3′-diaminobenzidine-tetrahydrochloride (DAB) chromogen/substrate kit (Abcam, Cambridge, UK). The staining of RhoB, occludin, and ZO-1 were evaluated by two independent investigators using bright-field light microscopy.

2.3. In situ hybridization (ISH)

The *in situ* detection of miR-21 was performed using 5-μm FFPE sections of specimens from cohort 2 with a 5′-end digoxigenin-labeled Locked Nucleic Acid (LNA)-modified mirCURY miR-21 detection probe (Exiqon, Vedbaek, Denmark). A probe specific for U6 small nuclear RNA (Exiqon, Vedbaek, Denmark) was used as positive control. Briefly, after deparaffinization, the sections were subjected to proteinase K (20 μg/ml) digestion for 20 min, and the postfixed tissues were subsequently incubated overnight with the probes. For immunodetection, the tissues were incubated overnight at 4 °C with anti-DIG-AP FAB fragments conjugated to alkaline phosphatase (1/2000; Roche, Mannheim, Germany). The final visualization was performed with nitro blue tetrazolium/5-bromo-4-chloro-3-indolyl phosphate (NBT/BCIP, Sigma–Aldrich, MO, USA) solution. The slides were counterstained with nuclear fast red to visualize the nuclei. The sections were examined separately by two independent investigators.

2.4. Cell culture

The human colonic epithelial-like cancer cell line Caco-2 was obtained from the Cell Institute Affiliated China Science Research Institute (Shanghai, China). The cells were maintained at a density of 1×10^5 cells/ml in DMEM containing 10% fetal bovine serum and a 1% antibiotic–antimycotic solution under standard cell culture conditions at 37 °C in a humidified 5% CO_2 incubator.

2.5. RNA oligoribonucleotides and cell transfection

miR-21 mimics, mimics control, siRNA targeting RhoB coding sequences (siRNA-RhoB, 5′-GAACTATGTGGCCGACATT-3′), and an siRNA-RhoB negative control (siRNA-RhoB NC, 5′-TACACATGTGTGTGACACG-3′) were chemically synthesized by GenePharma (Shanghai, China). Transfection was performed with the Lipofectamine 2000 reagent (Invitrogen, Carlsbad, CA, USA) according to the manufacturer's instructions. For each transfection, a final concentration of 50 nM of RNA mimics or 100 nM of siRNA and their respective negative controls were used.

2.6. Ultrastructural analysis

The morphological evaluation of TJs in the Caco-2 cells was performed using transmission electron microscopy (TEM) analysis. Briefly, after transfection, cells were fixed with 2% glutaraldehyde and postfixed with 1% osmium tetroxide in PBS and incubated at 4 °C for 2 h. The samples were then placed at 4 °C overnight and stained with 3% uranyl acetate (2 h). After passing through a series of solutions with increasing alcohol concentration, the samples were immersed in propylene oxide (10 min), immersed in equal parts propylene oxide and epoxy resin (2 h), incubated overnight in pure resin, and then embedded in resin molds at 60 °C for 2 days. Semi-thin sections (0.5 μm) stained with toluidine blue were examined using a light microscope to pre-select the most important areas. Lastly, ultrathin sections (80 nM) were cut using an LKB-V (Philip, Eindhoven, Netherlands); the sections were placed on copper grids, treated with lead citrate, and observed and photographed using a CM-120 (Philip, Eindhoven, Netherlands) TEM.

2.7. Measurement of TER and FITC-inulin flux

Caco-2 cells were seeded on to 24-well transwell inserts (Corning, NY, USA) for the assays. TER was measured by using a Millicell-ERS electrical resistance system (Millipore, Bedford, MA, USA). TER ($\Omega\ cm^2$) = (Total resistance (Ω) − Blank resistance (Ω)) × Area (cm^2). Paracellular flux assay was measured by incubating cell monolayers in the presence of FITC-inulin (500 μg/ml, Sigma) in the apical chamber. After 2 days incubation at 37 °C, aliguots of the apical and basal medium were sampled, and the fluorescence level was measured by using a spectrofluorometer (Fluoroskan Ascent FL, Thermo Labsystem, USA). The flux of FITC-inulin into the basal well was calculated as the percentage of total fluorescence administered into the apical well per hour per cm^2 surface area.

2.8. Real-time RT-PCR analysis of mRNA and miRNA expression

The isolation of total RNA from serum, tissues of patients or Caco-2 cells was performed using the Trizol reagent (Invitrogen, Carlsbad, CA, USA) for both the miRNA and mRNA analyses. Stem-loop quantitative PCR was performed for the analysis of mature miR-21 expression using the miScript PCR System (Qiagen, Hilden, Germany) with the 7900 Real-Time PCR system. The relative expression was calculated by the comparative CT method and normalized to the expression of U6 small nuclear RNA. RhoB mRNA was quantified by qRT-PCR using the Quantitect SYBR Green PCR Kit (Qiagen). A GAPDH endogenous control was used for normalization. The relative transcript level of each gene was calculated by the change in threshold ($2^{-\Delta\Delta CT}$) method.

2.9. Western Blot analysis

The total protein from the specimens and cultured cells was obtained by cell lysis using the M-PER Mammalian Protein Extraction Reagent (Pierce Biotechnology Inc., Rockford, IL, USA). The protein concentration was determined using the BCA protein assay kit (Pierce Biotechnology Inc.) with BSA as the standard. The proteins (100 μg) were separated by SDS–polyacrylamide gel electrophoresis and transferred onto polyvinylidene difluoride membranes (Millipore Co., Bedford, MA, USA). After blocking with 5% non-fat milk in TBS with 0.05% Tween-20 (TBST) at room temperature for 2 h, the membranes were incubated at 4 °C overnight with the primary antibodies. The proteins were visualized using an enhanced chemiluminescence Western Blot substrate (Pierce Biotechnology Inc.). Primary antibodies against the following proteins were used: RhoB, occludin and ZO-1. GAPDH was used as an internal control.

2.10. Statistical analysis

Quantitative variables were analyzed using the Student's *t*-test and the Mann–Whitney *U* test; qualitative variables were analyzed using either the chi-square test or Fisher's test. Comparisons among multiple groups were performed using a one-way analysis of variables (ANOVA). The data are presented as the mean ± standard deviation (SD) from at least three separate experiments. The confidence intervals (CI) throughout the study were set at 95%. A two-sided *P*-value of <0.05 was regarded as statistically significant. The statistical analyses were performed using the GraphPad Prism software (Version 5.01, GraphPad, San Diego, CA) and the SAS System for Windows software (version 8.02, Cary, North Carolina, USA).

3. Results

3.1. Both the mucosal and serum levels of miR-21 were upregulated in patients with chronic UC

First, we sought to determine whether miR-21 is differentially expressed under physiologic conditions and in chronic inflammation. Colon pinch biopsies were obtained from patients with

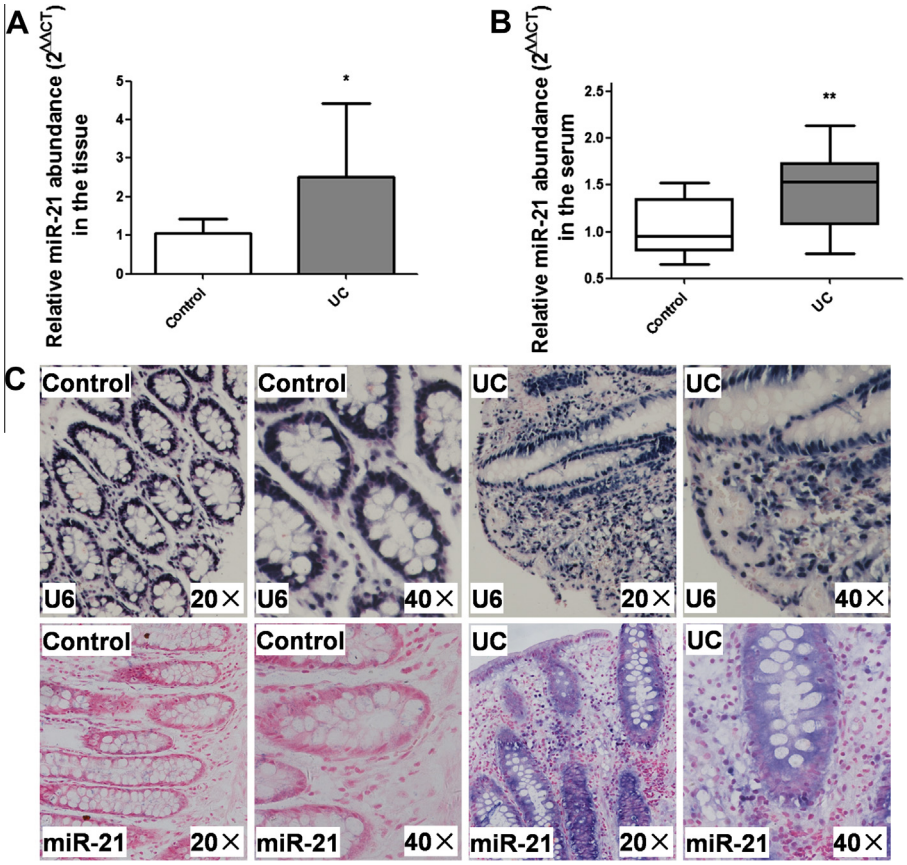

Fig. 1. Up-regulation of miR-21 levels in the colon and serum of UC patients and healthy controls. (A) Expression levels of miR-21 assessed by qRT-PCR in UC ($n = 15$) and normal colonic biopsies ($n = 15$). Bars, SD. $^{*}P < 0.05$. (B) Expression levels of miR-21 by qRT-PCR in the serum of UC patients ($n = 15$) compared with that of healthy subjects ($n = 15$). The data are presented as box-whisker plots (box, 25–75%; whisker, 5–95%; line, median). Bars, SD. $^{**}P < 0.01$. (C) Expression of miR-21 in UC and normal colonic biopsies using ISH analysis. The positive staining of epithelial cells appears as a blue–violet color, whereas the nuclei stain red. The pictures were imaged at 20× or 40× magnification. (For interpretation of the references to color in this figure legend, the reader is referred to the web version of this article.)

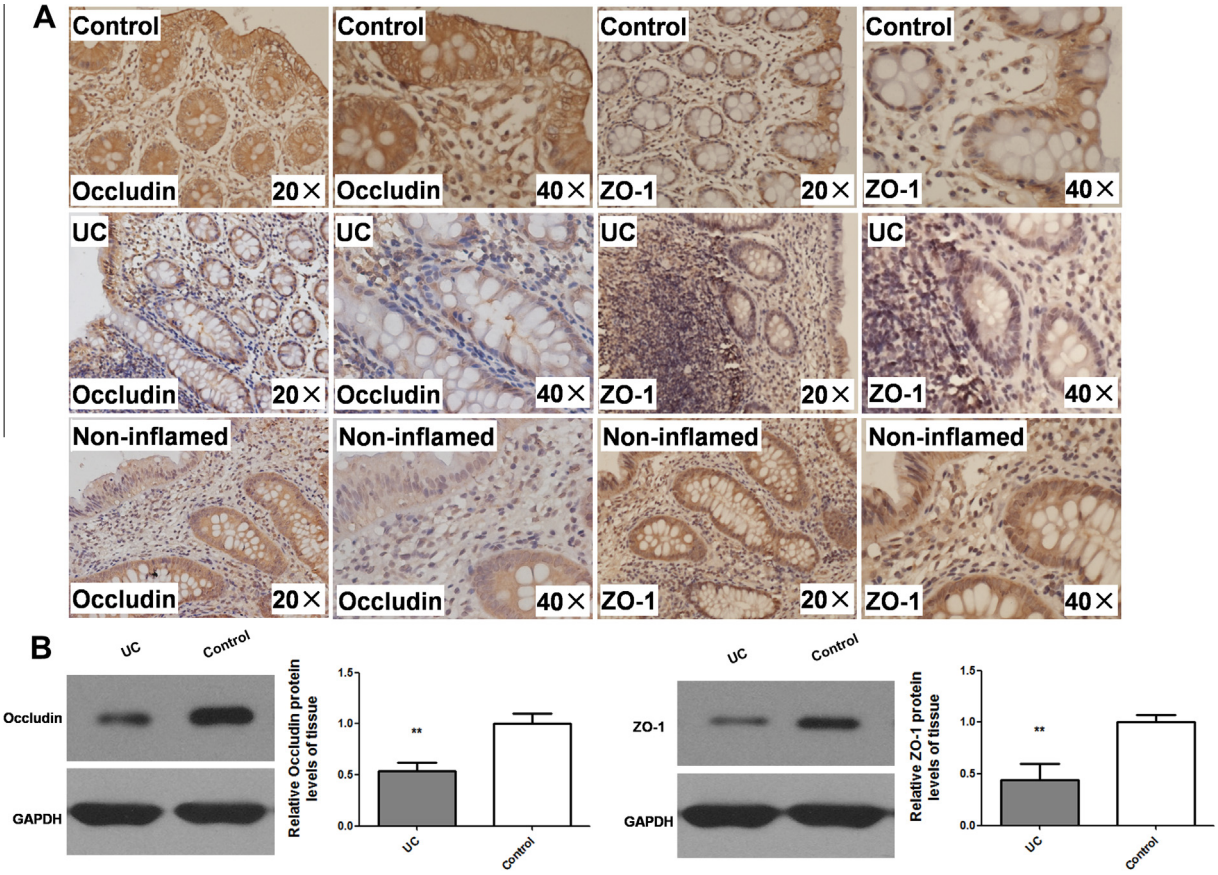

Fig. 2. Immunohistochemical and Western Blot analyses evaluating the expression of tight junction proteins. (A) Occludin and ZO-1 immunostaining of the UC colonic tissues, the non-inflamed colonic tissues in UC, and the healthy control colonic tissues. The pictures were imaged at 20× or 40× magnification. (B) Western Blot analysis showing representative images of the protein levels of occludin and ZO-1 in the UC and control colonic sections. The assays were performed in triplicate. Bars, SD. $^{**}P < 0.01$ compared with the PBS control.

zhistologically confirmed UC and normal, healthy control individuals. The clinical characteristics of each group are listed in Table 1.

qRT-PCR analysis was performed using samples from cohort 1, revealing that the expression of miR-21 was 2.4-fold (95% CI, 0.32–2.61) higher in the UC tissues than in normal colonic mucosa ($P < 0.05$; Fig. 1A). We also measured the levels of miR-21 in the serum of the control subjects and compared them with those from the patients with chronic UC. Again, there was a marked increase ($P < 0.01$; Fig. 1B) in the levels of miR-21 in the serum of the patients with UC.

3.2. ISH analysis for miR-21

Given the abundant expression of miR-21 in UC in cohort 1, we sought to identify the cellular localization of miR-21 by performing ISH on colon biopsy tissues from cohort 2 to better characterize the molecular pathways regulated by miR-21 in disease processes. Consistent with the results of the qRT-PCR from cohort 1, miR-21 expression was more abundant in the UC tissue, with a significant reduction observed in the control tissue (Fig. 1C). miR-21 was predominantly expressed in the epithelial cells in chronic UC tissues, whereas miR-21 expression appeared to be qualitatively lower in the epithelial layer in the normal colon.

3.3. Overexpression of miR-21 in patients with UC and Caco-2 cells impaired intestinal epithelial tight junction integrity and morphology

Immunohistochemical studies of the expression of such tight junction proteins as occludin and ZO-1 were performed using the 15 UC samples from cohort 1. Compared to the healthy control specimens and the non-inflamed colonic tissues in UC, we found that the staining of occludin and ZO-1 at the intercellular junctions was significantly weaker in the UC specimens (Fig. 2A). The Western Blot analysis (Fig. 2B) also showed decreased protein expression of occludin and ZO-1 in the UC colonic sections, compared to the healthy colonic tissues from cohort 2.

We next determined the effects of miR-21 on the intestinal epithelial barrier function in Caco-2 cell culture assays. Caco-2 cells were transfected with mimics of mature miR-21, and Western Blot analysis (Fig. 3A) revealed a loss of occludin and ZO-1 compared to the PBS or miR-21 mimics control.

At the ultrastructural level (Fig. 3B), microvilli were found on the apical cell surface, and a reduction or change in their appearance was noted in the miR-21-transfected cells. In addition, the miR-21-transfected group exhibited an irregular widening of the intercellular space, vacuolization, chromatin condensation, and even epithelial apoptosis.

Epithelial permeability was performed by measuring the TER and the FITC-inulin flux in Caco-2 cell monolayers. Transfection of miR-21 mimics into Caco-2 cells resulted in a decrease of the TER and an increase of the FITC-inulin flux compared with cells transfected with control group ($P < 0.01$; Fig. 4C and D).

3.4. RhoB and miR-21 expression were inversely correlated in vitro and in vivo

Because miR-21 has been widely reported to target RhoB [11–13] and because RhoB is also involved in modulating intestinal

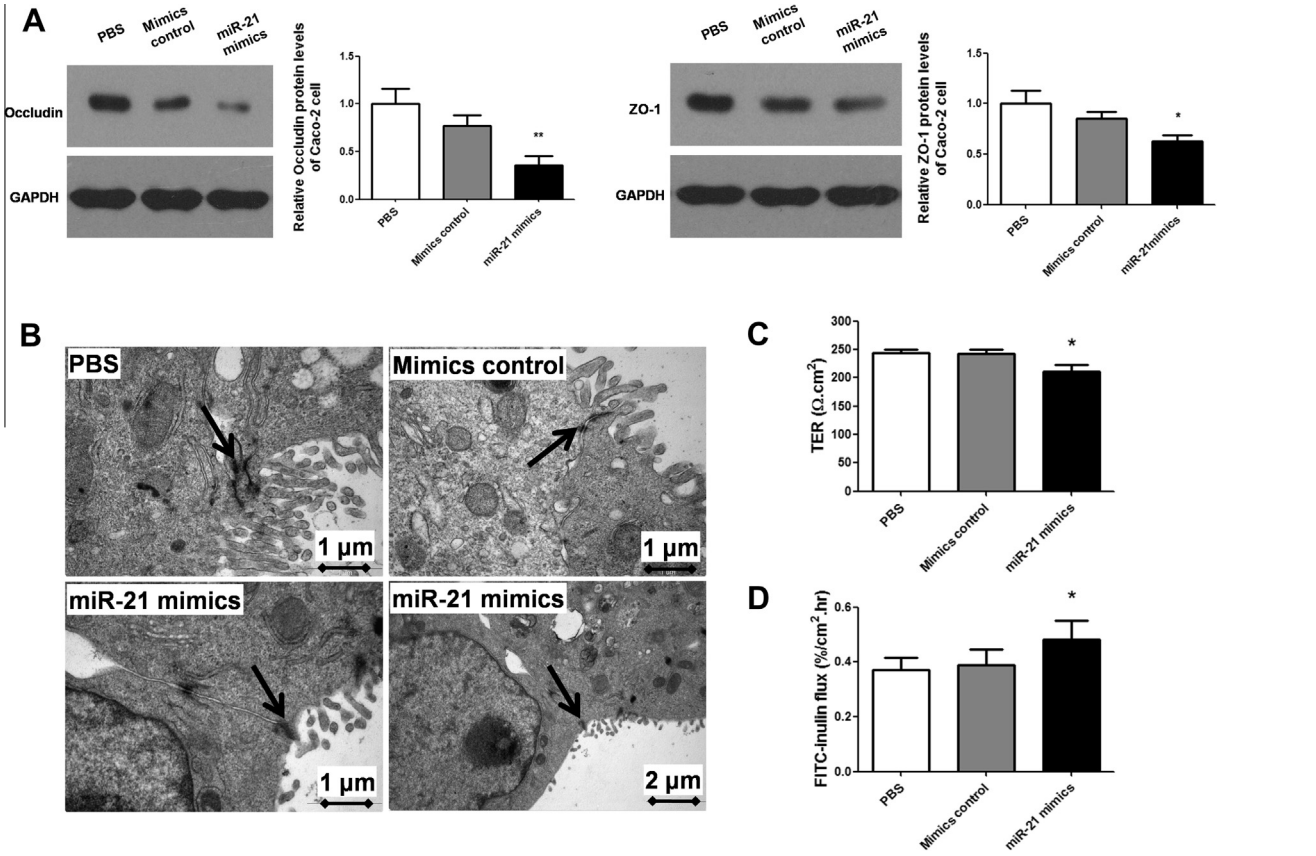

Fig. 3. Overexpression of miR-21 in Caco-2 cells impaired intestinal epithelial barrier function. (A) Western Blot analysis showing representative images of the protein levels of occludin and ZO-1 in miR-21 mimics-transfected and miR-21 mimics control-transfected Caco-2 cells and normal (PBS) Caco-2 cells. The assays were performed in triplicate. Bars, SD. $^{*}P < 0.05$ compared with the PBS control; $^{**}P < 0.01$ compared with the PBS control. (B) Ultrastructural characteristics of the Caco-2 cells transfected with PBS, miR-21 mimics control, or miR-21 mimics. The lateral surface is indicated with arrows. Bars, 1 μm: 35,000× magnification; 2 μm: 17,500× magnification. (C, D) Measurement of TER and FITC-inulin flux in the Caco-2 cells transfected with PBS, miR-21 mimics control, or miR-21 mimics. The assays were performed in triplicate. Bars, SD. $^{*}P < 0.05$ compared with the PBS control.

epithelial permeability [14,15], we then assayed the protein and mRNA levels of RhoB in colonic tissues and Caco-2 cells.

As shown by the immunohistochemical analysis (Fig. 4A) and Western Blot analysis (Fig. 4B), the colonic RhoB protein level was significantly decreased in the patients with UC. To confirm that transfected miR-21 was successfully delivered into the Caco-2 cells and that it suppressed the expression of RhoB, we evaluated the miR-21 and RhoB mRNA and protein levels by qRT-PCR analysis and Western Blot analysis, respectively. The results showed that the RhoB mRNA ($P < 0.01$) and protein levels were inversely correlated with an increased accumulation of miR-21 in the miR-21-mimics-treated groups, compared to those transfected with PBS or the miR-21 mimics control (Fig. 4C). Similarly, as demonstrated by Western Blot analysis, the introduction of either miR-21 mimics or the siRNA-mediated depletion of RhoB in Caco-2 cells caused the downregulation of both RhoB and occludin expression (Fig. 4D). Decreased TER by siRNA-mediated depletion of RhoB was accompanied by increased permeability to inulin ($P < 0.01$; Fig. 4E and F), in accordance with the result of miR-21-transfected group.

4. Discussion

The intestinal epithelial barrier, a delicate structure composed of a single layer of epithelial cells, has evolved to maintain a balance between absorbing essential nutrients and preventing the entry of and response to hazardous substances [16]. Disruption of the gut mucosal barrier is a hallmark of IBD that leads to permeability defects, increased antigenic penetration, exacerbation of the underlying immune system, and subsequent tissue damage [5,17]. In contrast, enhancement of the TJ barrier prevents the development of gut inflammation [18].

There are recent reports on the role of miRNAs in the regulation of intestinal permeability. A previous study by Ye et al. indicated that miR-122a regulates intestinal TJ permeability by targeting occludin mRNA degradation [19]. Tang et al. reported that alcohol-induced miR-212 expression resulted in the disruption of the intestinal paracellular tight junctions by down-regulating ZO-1 translation [20]. McKenna et al. confirmed in mouse models that miRNAs play multiple important roles in the intestinal epithelium and that loss of intestinal miRNAs causes impaired epithelial barrier function, resulting in acute inflammation [21]. In the present study, we measured the miR-21 levels in serum samples of UC patients and found an increase ($P < 0.01$) in the levels of miR-21, a result that is supported by the findings in peripheral blood cell miRNAs in a study conducted by Paraskevi et al. [22]. Similar studies identifying a significant increase in miR-21 levels in the serum of patients with pediatric CD have been reported [23]. Therefore, circulating miRNA-21 can be regarded as a potential biomarker with clinical utility.

We confirmed that the mucosal levels of miR-21 were upregulated in patients with UC. Moreover, our results demonstrate the association between the elevation of miR-21 and impaired intestinal barrier function in patients with UC. We transfected Caco-2 cells with synthetic mimics of mature miR-21, which resulted in

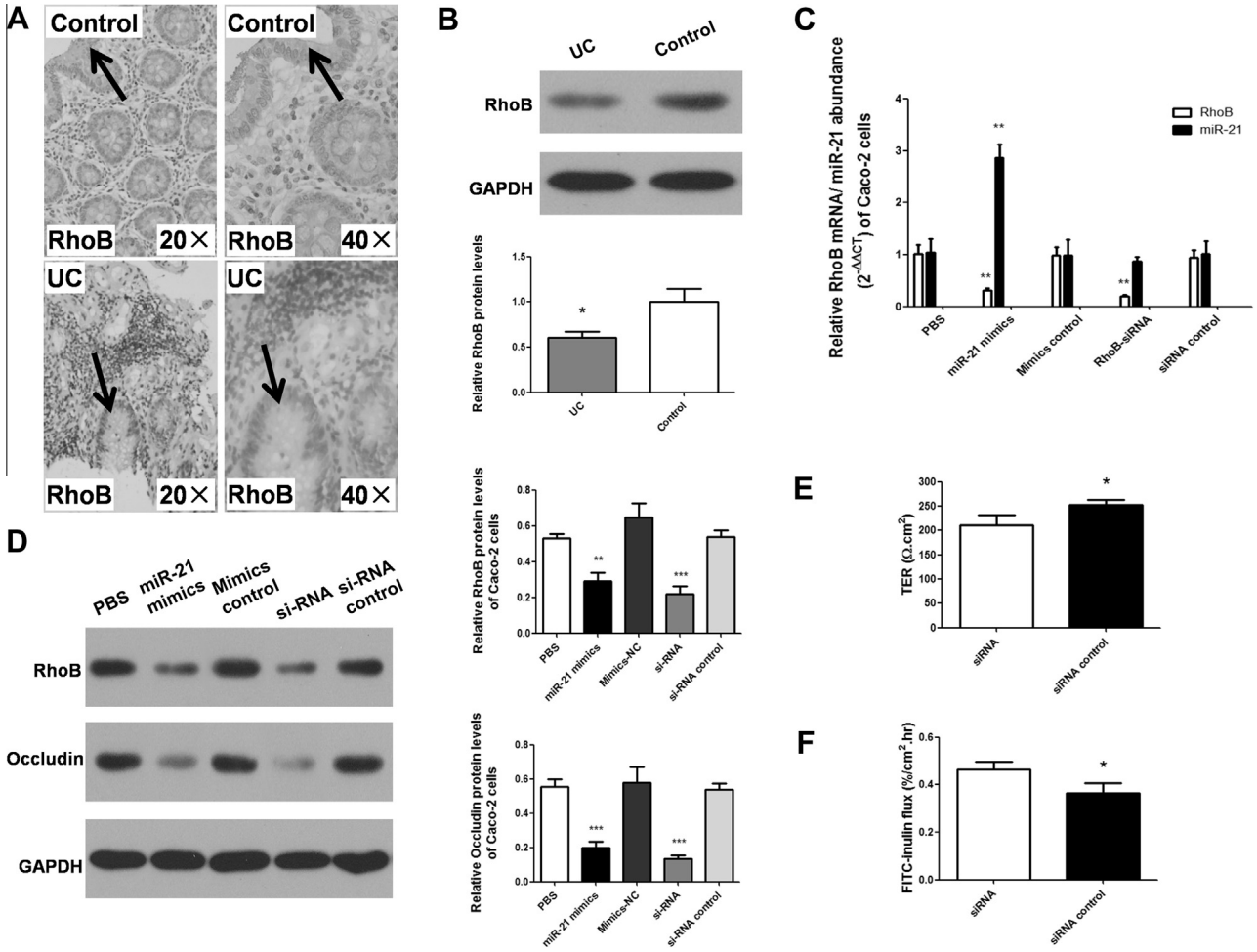

Fig. 4. The protein levels of RhoB in colonic tissues and Caco-2 cells. (A) Immunohistochemical analysis of RhoB in UC and healthy control colonic sections. The lateral surface is indicated with arrows. The slides were imaged at 20× or 40× magnification. (B) Western Blot analysis showing representative images of the protein levels of RhoB in the UC and control colonic sections. The assays were performed in triplicate. Bars, SD. $^{*}P < 0.05$ compared with the PBS control. (C) qRT-PCR analysis of RhoB mRNA in Caco-2 cells transfected with PBS, miR-21 mimics, miR-21 mimics control, RhoB siRNA, or siRNA control. $^{**}P < 0.01$ compared with the PBS control. (D) Western Blot analysis showing representative images of the protein levels of RhoB and occludin in Caco-2 cells. $^{**}P < 0.01$ compared with the PBS control; $^{***}P < 0.001$ compared with the PBS control. (E, F) Measurement of TER and FITC-inulin flux in the Caco-2 cells transfected with RhoB siRNA or siRNA control. The assays were performed in triplicate. Bars, SD. $^{*}P < 0.05$ compared with the siRNA control.

the loss of tight junction proteins and ultrastructural changes, compared to the control group.

To propose a putative mechanism for the role of miR-21 in the inhibition of intestinal barrier function, we focused on the identification of the targets of this miRNA. We employed two different computational programs, TargetScan (http://www.targetscan.org/) [24] and miRanda (http://www.microrna.org/) [25], to predict the targets of miR-21. Interestingly, RhoB, a member of the Ras superfamily of GTPases was identified. The subfamily of Rho GTPases consists of 22 members that can be divided into eight subclasses, all of which play important roles in the organization of the actin cytoskeleton and cell shape [26]. In contrast to its family members RhoA and RhoC, RhoB is known to act as a tumor suppressor that affects the cell cycle, angiogenesis, and apoptosis and regulates actin organization, cell migration, and cell adhesion [13,27]. In addition, via a luciferase reporter assay, RhoB was recently reported to be targeted by miR-21 in eight colorectal cancer cell lines [13], hepatocellular carcinoma cell lines [11], and human umbilical vein endothelial cells (HUVECs) [12]. Given that the RhoB mRNA contains one conserved binding site for miR-21 within the RhoB 3′UTR, we assayed the level of RhoB in colonic tissues and Caco-2 cells. Our results showed that levels of RhoB were reduced by the overexpression of miR-21 in the UC dysfunctional process. The transfection of either miR-21 oligonucleotide or RhoB-siRNA resulted in the decrease of the TER and an increase of the FITC-inulin flux. These data strongly support that overexpression of miR-21 impairs the intestinal epithelial tight junction by targeting RhoB.

In summary, this study demonstrates that miR-21 is upregulated in chronic UC. miR-21 induces the degradation of RhoB mRNA, leading to an increase in intestinal epithelial permeability. Circulating miRNA-21 is considered to be a potential novel biomarker with clinical utility, a potential that will require confirmation in large validation groups.

Disclosure

All procedures were conducted in accordance with the Declaration of Helsinki. Informed consent was acquired from all patients, and the Institute Ethics Committee approved the study protocol.

Acknowledgments

This work was financially sponsored by grants from the National Natural Science Foundation of China (No. 81200264), the

State Key Program of National Natural Science of China (No. 81230057), the Shanghai Rising-Star Program (No. 11QA1404800), the National Natural Science Foundation of China (No. 81001069), the National High Technology Research and Development Program (863 Program) (No. 2009AA02Z118), and the National Basic Research Program of China (973 Program) (No. 2008CB517403).

References

[1] E.V. Loftus Jr., Clinical epidemiology of inflammatory bowel disease: Incidence, prevalence, and environmental influences, Gastroenterology 126 (2004) 1504–1517.
[2] J.R. Pekow, J.H. Kwon, MicroRNAs in inflammatory bowel disease, Inflamm. Bowel Dis. 18 (2012) 187–193.
[3] I. Ordas, L. Eckmann, M. Talamini, D.C. Baumgart, W.J. Sandborn, Ulcerative colitis, Lancet 380 (2012) 1606–1619.
[4] A.H. Gitter, F. Wullstein, M. Fromm, J.D. Schulzke, Epithelial barrier defects in ulcerative colitis: characterization and quantification by electrophysiological imaging, Gastroenterology 121 (2001) 1320–1328.
[5] S.Y. Salim, J.D. Soderholm, Importance of disrupted intestinal barrier in inflammatory bowel diseases, Inflamm. Bowel Dis. 17 (2011) 362–381.
[6] D.P. Bartel, MicroRNAs: genomics, biogenesis, mechanism, and function, Cell 116 (2004) 281–297.
[7] F.J. Sheedy, E. Palsson-McDermott, E.J. Hennessy, C. Martin, J.J. O'Leary, Q. Ruan, D.S. Johnson, Y. Chen, L.A. O'Neill, Negative regulation of TLR4 via targeting of the proinflammatory tumor suppressor PDCD4 by the microRNA miR-21, Nat. Immunol. 11 (2010) 141–147.
[8] M. Fabbri, A. Paone, F. Calore, R. Galli, E. Gaudio, R. Santhanam, F. Lovat, P. Fadda, C. Mao, G.J. Nuovo, N. Zanesi, M. Crawford, G.H. Ozer, D. Wernicke, H. Alder, M.A. Caligiuri, P. Nana-Sinkam, D. Perrotti, C.M. Croce, MicroRNAs bind to Toll-like receptors to induce prometastatic inflammatory response, Proc. Natl. Acad. Sci. USA 109 (2012) E2110–2116.
[9] F. Wu, M. Zikusoka, A. Trindade, T. Dassopoulos, M.L. Harris, T.M. Bayless, S.R. Brant, S. Chakravarti, J.H. Kwon, MicroRNAs are differentially expressed in ulcerative colitis and alter expression of macrophage inflammatory peptide-2 alpha, Gastroenterology 135 (2008) 1624–1635. e1624.
[10] T. Takagi, Y. Naito, K. Mizushima, I. Hirata, N. Yagi, N. Tomatsuri, T. Ando, Y. Oyamada, Y. Isozaki, H. Hongo, K. Uchiyama, O. Handa, S. Kokura, H. Ichikawa, T. Yoshikawa, Increased expression of microRNA in the inflamed colonic mucosa of patients with active ulcerative colitis, J. Gastroenterol. Hepatol. 25 (Suppl. 1) (2010) S129–133.
[11] E.C. Connolly, K. Van Doorslaer, L.E. Rogler, C.E. Rogler, Overexpression of miR-21 promotes an in vitro metastatic phenotype by targeting the tumor suppressor RHOB, Mol. Cancer. Res. 8 (2010) 691–700.
[12] C. Sabatel, L. Malvaux, N. Bovy, C. Deroanne, V. Lambert, M.L. Gonzalez, A. Colige, J.M. Rakic, A. Noel, J.A. Martial, I. Struman, MicroRNA-21 exhibits antiangiogenic function by targeting RhoB expression in endothelial cells, PLoS ONE 6 (2011) e16979.
[13] M. Liu, Q. Tang, M. Qiu, N. Lang, M. Li, Y. Zheng, F. Bi, MiR-21 targets the tumor suppressor RhoB and regulates proliferation, invasion and apoptosis in colorectal cancer cells, FEBS Lett. 585 (2011) 2998–3005.
[14] M.R. Popoff, B. Geny, Multifaceted role of Rho, Rac, Cdc42 and Ras in intercellular junctions, lessons from toxins, Biochim. Biophys. Acta 1788 (2009) 797–812.
[15] A. Nusrat, M. Giry, J.R. Turner, S.P. Colgan, C.A. Parkos, D. Carnes, E. Lemichez, P. Boquet, J.L. Madara, Rho protein regulates tight junctions and perijunctional actin organization in polarized epithelia, Proc. Natl. Acad. Sci. USA 92 (1995) 10629–10633.
[16] Y. Goto, H. Kiyono, Epithelial barrier: an interface for the cross-communication between gut flora and immune system, Immunol. Rev. 245 (2012) 147–163.
[17] M.A. McGuckin, R. Eri, L.A. Simms, T.H. Florin, G. Radford-Smith, Intestinal barrier dysfunction in inflammatory bowel diseases, Inflamm. Bowel Dis. 15 (2009) 100–113.
[18] M.C. Arrieta, K. Madsen, J. Doyle, J. Meddings, Reducing small intestinal permeability attenuates colitis in the IL10 gene-deficient mouse, Gut 58 (2009) 41–48.
[19] D. Ye, S. Guo, R. Al-Sadi, T.Y. Ma, MicroRNA regulation of intestinal epithelial tight junction permeability, Gastroenterology 141 (2011) 1323–1333.
[20] Y. Tang, A. Banan, C.B. Forsyth, J.Z. Fields, C.K. Lau, L.J. Zhang, A. Keshavarzian, Effect of alcohol on miR-212 expression in intestinal epithelial cells and its potential role in alcoholic liver disease, Alcohol. Clin. Exp. Res. 32 (2008) 355–364.
[21] L.B. McKenna, J. Schug, A. Vourekas, J.B. McKenna, N.C. Bramswig, J.R. Friedman, K.H. Kaestner, MicroRNAs control intestinal epithelial differentiation, architecture, and barrier function, Gastroenterology 139 (2010) 1654–1664. e1651.
[22] A. Paraskevi, G. Theodoropoulos, I. Papaconstantinou, G. Mantzaris, N. Nikiteas, M. Gazouli, Circulating MicroRNA in inflammatory bowel disease, J. Crohns Colitis 6 (2012) 900–904.
[23] A.M. Zahm, M. Thayu, N.J. Hand, A. Horner, M.B. Leonard, J.R. Friedman, Circulating microRNA is a biomarker of pediatric Crohn disease, J. Pediatr. Gastroenterol. Nutr. 53 (2011) 26–33.
[24] B.P. Lewis, C.B. Burge, D.P. Bartel, Conserved seed pairing, often flanked by adenosines, indicates that thousands of human genes are microRNA targets, Cell 120 (2005) 15–20.
[25] P. Sethupathy, M. Megraw, A.G. Hatzigeorgiou, A guide through present computational approaches for the identification of mammalian microRNA targets, Nat. Methods 3 (2006) 881–886.
[26] P. Aspenstrom, A. Fransson, J. Saras, Rho GTPases have diverse effects on the organization of the actin filament system, Biochem. J. 377 (2004) 327–337.
[27] F.M. Vega, A. Colomba, N. Reymond, M. Thomas, A.J. Ridley, RhoB regulates cell migration through altered focal adhesion dynamics, Open Biol. 2 (2012) 120076.